



**SOUTHERN PLAINS**  
TRANSPORTATION CENTER

## **Degradation of Mechanically Stabilized Earth Reinforcements Exposed to Different Environmental Conditions**

Luisa Morales  
Yadira Calderas  
Arturo Bronson, Ph. D.

**SPTC15.1-46-F**

**Southern Plains Transportation Center  
201 Stephenson Parkway, Suite 4200  
The University of Oklahoma  
Norman, Oklahoma 73019**

## **Disclaimer**

*The contents of this report reflect the views of the authors, who are responsible for the facts and accuracy of the information presented herein. This document is disseminated under the sponsorship of the Department of Transportation University Transportation Centers Program, in the interest of information exchange. The U.S. Government assumes no liability for the contents or use thereof.*

## Technical Report Documentation Page (TRDP)

1. REPORT NO <b>SPTC15.1-46-F</b>	2. GOVERNMENT ACCESSION NO.	3. RECIPIENTS CATALOG NO.	
4. TITLE AND SUBTITLE <b>Degradation of Mechanically Stabilized Earth Reinforcements Exposed to Different Environmental Conditions</b>		5. REPORT DATE <b>November 30, 2019</b>	
		6. PERFORMING ORGANIZATION CODE	
7. AUTHOR(S) <b>L. Morales, Y. Calderas and A. Bronson</b>		8. PERFORMING ORGANIZATION REPORT	
9. PERFORMING ORGANIZATION NAME AND ADDRESS <b>Center for Transportation Infrastructure Systems (CTIS) University of Texas at El Paso 500 West University Ave. El Paso, Texas 79968</b>		10. WORK UNIT NO.	
		11. CONTRACT OR GRANT NO. <b>DTRT13-G-UTC36</b>	
12. SPONSORING AGENCY NAME AND ADDRESS <b>Southern Plains Transportation Center 201 Stephenson Pkwy, Suite 4200 The University of Oklahoma Norman, OK 73019</b>		13. TYPE OF REPORT AND PERIOD COVERED <b>Final November 1, 2016 – Nov 30, 2019</b>	
		14. SPONSORING AGENCY CODE	
15. SUPPLEMENTARY NOTES <b>University Transportation Center</b>			
16. ABSTRACT <p>Mechanically stabilized earth (MSE) reinforcements composed usually of galvanized steel are embedded in soils varying in corrosion susceptibility depending primarily on the concentration of chloride and sulfate ions within the pores of the soil or even the water collected in the backfill. Linear Polarization Resistance (LPR) and Tafel slopes were used to determine corrosion rate of galvanized steel immersed in KCl (i.e., 0.1 mM to 0.1 M) solutions and sometimes having 0.1 mM K<sub>2</sub>SO<sub>4</sub> content. Three techniques were used to calculate the corrosion rate – one with the Tafel slopes within 130 mV range of the E<sub>corr</sub> (denoted as Tafel), the second method combined with Tafel slopes determined within 130 mV of E<sub>corr</sub> and LPR (labeled as LPR CR) and the third method used the Tafel slopes within 110 mV range from E<sub>corr</sub> combined with LPR (labeled as LPR CR selected). The three techniques determined consistent corrosion rates of galvanized steel with resistivity though the potential range selected of the Tafel slope seems to affect slightly the corrosion rate calculated.</p> <p>In addition, the atmospheric condition of the solution affected slightly the corrosion rate of the galvanized steel for stagnant, stirred and N<sub>2</sub> injected solutions. If one considers the stagnant solution as a baseline, the drawing of air into the solution will have more dissolved oxygen affecting Zn oxidation, or the anodic reaction, and decreased the mass transfer of oxygen enabling the dissolved oxygen in the solution to increase slightly for the cathodic reaction.</p>			
17. KEY WORDS <b>Mechanically Stabilized Earth, Corrosion, Galvanized Steel, Chlorides, Sulfates and Reinforcements</b>		18. DISTRIBUTION STATEMENT <b>No restrictions. This publication is available at <a href="http://www.sptc.org">www.sptc.org</a> and from the NTIS.</b>	
19. SECURITY CLASSIF. (OF THIS REPORT) <b>Unclassified</b>	20. SECURITY CLASSIF. (OF THIS PAGE) <b>Unclassified</b>	21. NO. OF PAGES <b>34</b>	22. PRICE

# SI\* (MODERN METRIC) CONVERSION FACTORS

## APPROXIMATE CONVERSIONS TO SI UNITS

SYMBOL	WHEN YOU KNOW	MULTIPLY BY	TO FIND	SYMBOL
<b>LENGTH</b>				
in	inches	25.4	millimeters	mm
ft	Feet	0.305	meters	m
yd	yards	0.914	meters	m
mi	miles	1.61	kilometers	km
<b>AREA</b>				
in <sup>2</sup>	square inches	645.2	square millimeters	mm <sup>2</sup>
ft <sup>2</sup>	square feet	0.093	square meters	m <sup>2</sup>
yd <sup>2</sup>	square yard	0.836	square meters	m <sup>2</sup>
ac	acres	0.405	hectares	ha
mi <sup>2</sup>	square miles	2.59	square kilometers	km <sup>2</sup>
<b>VOLUME</b>				
fl oz	fluid ounces	29.57	milliliters	mL
gal	gallons	3.785	liters	L
ft <sup>3</sup>	cubic feet	0.028	cubic meters	m <sup>3</sup>
yd <sup>3</sup>	cubic yards	0.765	cubic meters	m <sup>3</sup>
NOTE: volumes greater than 1000 L shall be shown in m <sup>3</sup>				
<b>MASS</b>				
oz	ounces	28.35	grams	g
lb	pounds	0.454	kilograms	kg
T	short tons (2000 lb)	0.907	megagrams (or "metric ton")	Mg (or "t")
<b>TEMPERATURE (exact degrees)</b>				
°F	Fahrenheit	5 (F-32)/9 or (F-32)/1.8	Celsius	°C

## APPROXIMATE CONVERSIONS FROM SI UNITS

SYMBOL	WHEN YOU KNOW	MULTIPLY BY	TO FIND	SYMBOL
<b>LENGTH</b>				
mm	millimeters	0.039	inches	in
m	meters	3.28	feet	ft
m	meters	1.09	yards	yd
km	kilometers	0.621	miles	mi
<b>AREA</b>				
mm <sup>2</sup>	square millimeters	0.0016	square inches	in <sup>2</sup>
m <sup>2</sup>	square meters	10.764	square feet	ft <sup>2</sup>
m <sup>2</sup>	square meters	1.195	square yards	yd <sup>2</sup>
ha	hectares	2.47	acres	ac
km <sup>2</sup>	square kilometers	0.386	square miles	mi <sup>2</sup>
<b>VOLUME</b>				
mL	milliliters	0.034	fluid ounces	fl oz
L	liters	0.264	gallons	gal
m <sup>3</sup>	cubic meters	35.314	cubic feet	ft <sup>3</sup>
m <sup>3</sup>	cubic meters	1.307	cubic yards	yd <sup>3</sup>
<b>MASS</b>				
g	grams	0.035	ounces	oz
kg	kilograms	2.202	pounds	lb
Mg (or "t")	megagrams (or "metric ton")	1.103	short tons (2000 lb)	T
<b>TEMPERATURE (exact degrees)</b>				
°C	Celsius	1.8C+32	Fahrenheit	°F

\*SI is the symbol for the International System of Units. Appropriate rounding should be made to comply with Section 4 of ASTM E380. (Revised March 2003)

## **Acknowledgements**

The researchers gratefully acknowledge the support of the Southern Plains Transportation Center with Dr. Dominique M. Pittenger at University of Oklahoma and Dr. Imad Abdallah of the Center for Transportation Infrastructure Systems in overseeing administrative matters. The technical discussions with Drs. Soheil Nazarian and Shane Walker at the University of Texas at El Paso, as well as Dr. Kenneth Fishman of McMahon & Mann Consulting Engineers, P.C., are also acknowledged.

**Degradation of Mechanically Stabilized Earth  
Reinforcements Exposed to Different Environmental  
Conditions**

**Final Report**

**November 2019**

**Luisa Morales, M.S. Engineering Graduate  
Yadira Calderas, Engineering Undergraduate  
Arturo Bronson, Ph. D. and Professor**

**Southern Plains Transportation Center  
201 Stephenson Pkwy, Suite 4200  
The University of Oklahoma**



## Table of Contents

Report Cover (added by SPTC .....	1
Disclaimer .....	i
Technical Report Documentation Page (TRDP).....	ii
Acknowledgements .....	iv
Table of Contents.....	i
List of Tables.....	iv
Executive Summary .....	v
Introduction .....	1
Problem Statement.....	2
Objective.....	2
Research Methodology and Scope of Work .....	2
Results and Discussion .....	5
Acquisition of Linear Polarization Resistance .....	5
Acquisition of Tafel Data.....	9
Analysis Relating Resistivity to Corrosion Rate .....	12
Summary.....	18
Implementation/Technology Transfer (if applicable).....	19
References.....	20
Appendix .....	22

## List of Figures

Figure - 1 Tafel plot characteristics: Bottom curve is the cathodic side and top curve is the anodic side .....	3
Figure 2 - Corrosion cell consists of a $K_2SO_4$ solution poured inside the reference electrode chamber containing the counter electrode and reference electrode separated by glass frit from the electrolytic solution.....	4
Figure 3 - Four trials of LPR measurements for a 0.1 mM $K_2SO_4$ - 1 mM KCl Solution ..	6
Figure 4 - LPR Plots for 0.1 mM $K_2SO_4$ - 0.1 mM KCl for a stagnant, stirred and $N_2$ injected .....	7
Figure 5. - The effect of KCl content additions on the LPR measurement in a stagnant 0.1 mM $K_2SO_4$ stagnant solution .....	7
Figure 6. - The effect of KCl content on the LPR measurement in a stirred 0.1 mM $K_2SO_4$ solution.....	7
Figure 7 - The effect of KCl solution on the LPR measurement in a 0.1 mM $K_2SO_4$ solution injected with $N_2$ .....	8
Figure 8 - Comparison of stagnant, stirred and $N_2$ injected solutions for KCl- 0.1 mM $K_2SO_4$ solutions.....	8
Figure 9. - Four trials of a Tafel plot 0.1 mM $K_2SO_4$ - 0.1 mM KCl for a stirred condition	9
Figure 10 - Four trials of a Tafel plot 0.1 mM $K_2SO_4$ - 0.1 mM KCl for a stirred condition .....	10
Figure 11 - Tafel plots comparison of changing atmosphere by having a stagnant, stirred and $N_2$ injected 0.1 mM $K_2SO_4$ - 0.1 mM KCl solution.....	11
Figure 12. - The effect of KCl solution on the Tafel plot in a stagnant 0.1 mM $K_2SO_4$ solution.....	11
Figure 13 - The effect of KCl solution on the Tafel plot in a 0.1 mM $K_2SO_4$ solution injected with $N_2$ .....	12
Figure 14 - Comparison of stagnant, stirred and $N_2$ injected solutions for KCl- 0.1 mM $K_2SO_4$ solutions.....	12
Figure 15 - The effect of KCl content on the resistivity of a stagnant solution KCl- 0.1Mm $K_2SO_4$ solutions.....	14



Figure 16 - The effect of KCl content on the corrosion rate determined with Tafel, and LPR techniques for stagnant KCl- 0.1 Mm K<sub>2</sub>SO<sub>4</sub> solutions ..... 14

Figure 17 - The correlation of the resistivity with the corrosion rate of stagnant KCl- 0.1mM K<sub>2</sub>SO<sub>4</sub> solutions..... 15

Figure 18 - The effect of KCl content on the resistivity of a KCl - 0.1 mM K<sub>2</sub>SO<sub>4</sub> stirred solutions..... 15

Figure 19. - The correlation of the resistivity with the corrosion rate determined with Tafel and LPR techniques for stirred KCl- 0.1mM K<sub>2</sub>SO<sub>4</sub> solutions injected with N<sub>2</sub> ..... 16

Figure 20 - The effect of KCl content on the resistivity of a KCl molarity- 0.1 mM K<sub>2</sub>SO<sub>4</sub> injected N<sub>2</sub> solutions..... 16

Figure 21 - The correlation of the resistivity with the corrosion rate determined with Tafel and LPR techniques for stirred KCl- 0.1mM K<sub>2</sub>SO<sub>4</sub> solutions injected with N<sub>2</sub> ..... 17

## List of Tables

Table 1. Tafel corrosion rates dependent on gas flushing conditions.....	22
Table 2. Average Tafel corrosion rates for every condition and molarity .....	22
Table 3. LPR Data: maximum range of 110 millivolts.....	23
Table 4. LPR Data: maximum range of 130 millivolts.....	23

## Executive Summary

Mechanically stabilized earth (MSE) reinforcements composed usually of galvanized steel are embedded in soils varying in corrosion susceptibility depending primarily on the concentration of chloride and sulfate ions within the pores of the soil or even the water collected in the backfill. Though the galvanized steel is predicted to corrode over several decades because of the low chloride and sulfate contents (e.g., < 400 mg/kg), the objective of this study was to relate the corrosion rate of galvanized steel with resistivity of chloride and sulfate solutions, as well as with and without its aeration. Linear Polarization Resistance (LPR) and Tafel slopes were used to determine corrosion rate of galvanized steel immersed in KCl (i.e., 0.1 mM to 0.1 M) solutions and sometimes having 0.1 mM K<sub>2</sub>SO<sub>4</sub> content. Three techniques were used to calculate the corrosion rate – one with the Tafel slopes within 130 mV range of the  $E_{\text{corr}}$  (denoted as Tafel), the second method combined with Tafel slopes determined within 130 mV of  $E_{\text{corr}}$  and LPR (labeled as LPR CR) and the third method used the Tafel slopes within 110 mV range from  $E_{\text{corr}}$  combined with LPR (labeled as LPR CR selected). The three techniques determined consistent corrosion rates of galvanized steel with resistivity though the potential range selected of the Tafel slope seems to affect slightly the corrosion rate calculated.

In addition, the atmospheric condition of the solution does affect slightly the corrosion rate of the galvanized steel for stagnant, stirred and N<sub>2</sub> injected solutions. If one considers the stagnant solution as a baseline, the drawing of air into the solution will increase its dissolved oxygen affecting Zn oxidation, or the anodic reaction, and decreases the mass transfer of oxygen enabling the dissolved oxygen in the solution to increase slightly for the cathodic reaction. Although the differential among the corrosion rates caused by the dissolved oxygen may establish macrocells along the length of the galvanized steel, the effect of macrocells on the overall corrosion needs further study to establish their relative contribution to the overall degradation.

## Introduction

Mechanically stabilized earth (MSE) wall structures are composed primarily of backfill materials and reinforcement consisting usually of galvanized steel strips. Though the estimated lifespan of galvanized steel in MSE walls may range from seventy-five to one-hundred years as reported by Elias et al. (2000) the galvanized steel degradation will depend on the soil chemistry, especially its chloride, sulfate and carbonate ion content within the MSE backfill. The fines are known to contain more sulfate and chloride contents that can be found at the bottom of an MSE structure causing the bottom strips of the wall to corrode sooner. The soil resistivity resulting from the moisture content is used as one of the parameters to characterize the soil chemistry prior to installing the MSE structure and during its lifespan.

Although soil resistivity usually is easily determined to assess the potential for corrosion of the galvanized steel, the resistivity must be correlated rigorously with the corrosion rate of galvanized steel embedded in soils or even immersed in chloride-sulfate solutions. In some corrosion studies, the galvanized steel is exposed to concentrated solutions with little linkage to the effect of diluted solutions containing aggressive anions (e.g., chloride and sulfate ions) on the corrosion rate. Since the galvanized steel used in the reinforcement of MSE walls are exposed to low chloride and sulfate contents (e.g., < 400 mg/kg) or less (i.e., for TX Department of Transportation limits,  $Cl^- \leq 100$  mg/kg or  $SO_4^{2-} \leq 200$  mg/kg) as reported by Borrok, Bronson and Nazarian (2013), studies of the corrosion rate of galvanized steel in diluted solutions are needed.

Gladstone et al. (1975) evaluated the loss rates for galvanized steel of MSE walls from 4 to 20 years and determined that the Zn corrosion rate was 15  $\mu\text{m}$  per year for the first year with subsequent years decreasing to 2  $\mu\text{m}$  per year. Galvanized steel corrodes in three stages -- Zn layer degrades first followed with Zn dissolution coupled to the surrounding Fe surface and finally the corrosion of the Fe. The stages were determined from a study of corrosion of galvanized steel immersed in chloride and sulfate aqueous solutions, as reported by El-Mahdy et al. (2000) and Yadav et al. (2004). Sagues et al. (2000) also reported on the contribution of localized corrosion and

the effects of electrochemical macrocells developed from differing soil characteristics near and away from the MSE wall.

### ***Problem Statement***

Mechanically stabilized earth (MSE) reinforcements composed primarily of galvanized steel are embedded in soils varying in corrosion susceptibility depending on the concentration of chloride and sulfate ions, which appear to segregate toward fines rather than coarse soils. The fines absorb more moisture than coarse soils and as a consequence, the chloride ion content in fines usually increases more than in coarse soils during water drainage. Irrespective of the location, the same corrosion formulae are used to estimate the corrosion of metallic reinforcement from the arid mountains of New Mexico to coastal regions of Louisiana. Given the vast environmental conditions of these regions, it is prudent to consider the impact of the available chloride and sulfate ion content within the collected water on the estimation of the corrosion rate of MSE reinforcements.

### ***Objective***

The objective of the present study was to relate the corrosion rate of the galvanized steel used for MSE reinforcement to the resistivity of chloride and sulfate mixture linked to its molarity. In this project, a chloride and sulfate mixture will be exposed to the galvanized strip, instead of soil, to manipulate the solution's molarity content. Though laboratory measurements were acquired at an accelerated pace, the corrosion rates would give an indication of the stages of dissolution of the galvanized steel.

### **Research Methodology and Scope of Work**

A quick and common technique for measuring the corrosion rate of metals is the linear polarization resistance (LPR), as reported by Oldham and Mansfeld (1973). Although they prefer to refer to the LPR as the polarization resistance, this technique perturbs the surface of the galvanized steel with a potential of  $\pm 10$  mV causing a current flow. The subsequent potential-current slope defines a polarization resistance ( $R_p$ ), i.e.,

$\Delta E/\Delta i=R_p$ , which is inversely proportional to the corrosion rate. The polarization resistance is supplemented with the Tafel slopes. The anodic and cathodic slopes ( $\beta_a$  and  $\beta_c$ , respectively) are acquired from the anodic and cathodic sides of the Tafel plot, as discussed by Jones (1992) and shown in Figure 1.

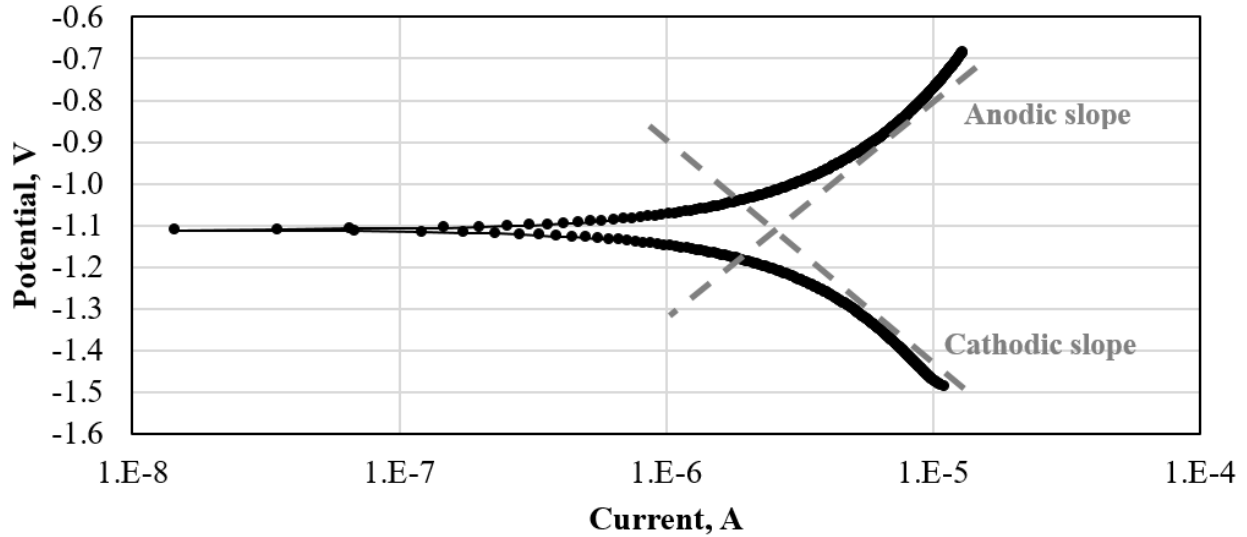


Figure - 1 Tafel plot characteristics: Bottom curve is the cathodic side and top curve is the anodic side

The polarization resistance is used to obtain corrosion rate of the galvanized steel with the Stern-Geary equation (1) below:

$$R_p = \frac{\Delta E}{\Delta i} = \frac{\beta_a \beta_c}{2.3 i_{corr} (\beta_a + \beta_c)} \quad (\text{eq.1})$$

The corrosion rate (CR) was calculated by using the current density. The current density is obtained from LPR or Tafel, and plugging it in to Faraday's Law reported by Fishman and Withiam (2011) as shown in the equation (2):

$$CR \left( \frac{\mu m}{yr} \right) = (3.27 \times 10^6) \times \frac{i_{corr} \times W}{\rho \times n} \quad (\text{eq.2})$$

To calculate the corrosion rate using Faraday's Law, the atomic weight of zinc (W) with 65.4 grams per mole, the density ( $\rho$ ) of zinc with 7.14 g/cm<sup>3</sup>, and the number of valance electrons (n) with 2 for zinc.

The corrosion apparatus consisted primarily of an electrochemical cell and an electrochemical potentiostat (Gamry 600 Instruments). The components of the cell included a cross section of galvanized steel as the working electrode (WE), titanium (Ti) rod as the counter electrode (CE), and Cu/CuSO<sub>4</sub> reference-electrode (RE), as shown in Figure 2. All electrodes were submerged into solutions prepared from reagent grade K<sub>2</sub>SO<sub>4</sub> and KCl crystals with deionized water. The electrolyte contained a mixture of potassium sulfate (K<sub>2</sub>SO<sub>4</sub>) with a molarity of one millimolar and potassium chloride (KCl) with a molarity ranging from one millimolar to 0.1 molar. The reference electrode is separated from the mixture by a glass frit with a porosity of 4-8 microns. The reference electrode chamber, or intermediate chamber, contains 1 millimolar (mM) K<sub>2</sub>SO<sub>4</sub> to minimize the poisoning of the RE by the chloride solution.

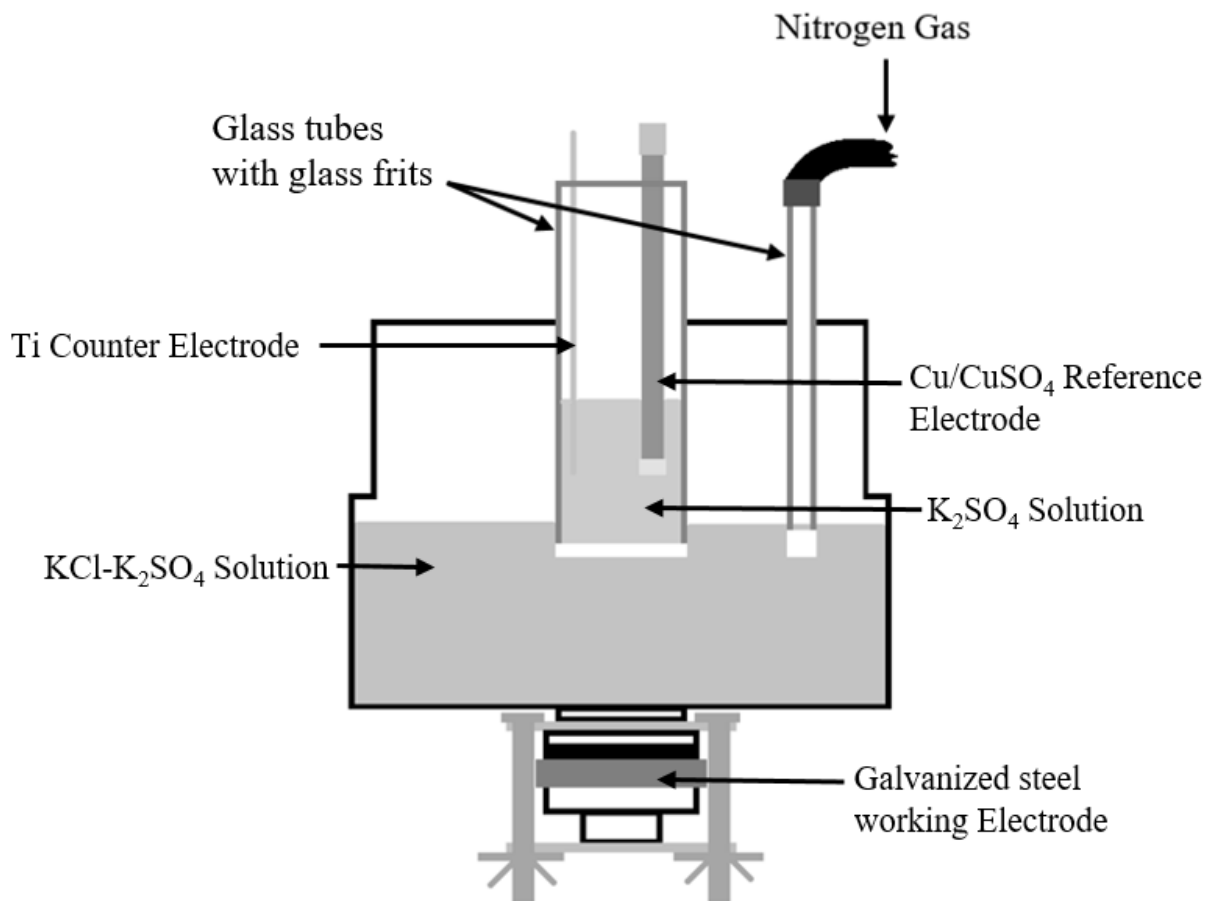


Figure 2 - Corrosion cell consists of a K<sub>2</sub>SO<sub>4</sub> solution poured inside the reference electrode chamber containing the counter electrode and reference electrode separated by glass frit from the electrolytic solution

Solutions of KCl and K<sub>2</sub>SO<sub>4</sub> were prepared by decreasing the molarity of KCl from 1 M to 1mM with a constant 1 mM K<sub>2</sub>SO<sub>4</sub> content. Electrodes were placed within the corrosion cell for ten minutes prior to initiating the electrochemical measurements. Linear polarization resistance and Tafel tests were performed at least three times for each molarity. For a set of experiments, nitrogen was bubbled into solutions through a glass frit, as shown in Figure 2. Again, nitrogen is injected into the solutions during the soaking time of ten minutes and continued throughout the electrochemical measurements. The last step is running the same test procedure by aerating the mixture. The mixture is poured to an opened beaker and placed into a magnetic stirrer. A magnetic bar is placed inside the beaker and the speed of the stirrer is adjusted. The solution is stirred for 30 minutes drawing the surrounding air atmosphere. Before running the tests, the solution is held inside the corrosion cell and in contact with the galvanized steel for ten minutes.

After the Tafel test, the conductivity of the solution was measured with a *COM-100 HM Digital EC TDS & Temperature Waterproof Meter* device. The reciprocal of conductivity converts to the resistivity of the solution, for which the latter is correlated with KCl content and corrosion rate.

## **Results and Discussion**

The electrochemical measurements acquired the linear polarization resistance and Tafel slopes, which were used to determine the corrosion rate of galvanized steel in chloride and chloride-sulfate solutions. In the following sections, the results of the polarization resistance are summarized first followed by the polarization scans used to determine the Tafel slopes. Both techniques were used to determine the corrosion rate, as described in the subsequent paragraphs.

### ***Acquisition of Linear Polarization Resistance***

For all measurements of linear polarization resistance, four trials were acquired as exemplified for the 0.1 mM K<sub>2</sub>SO<sub>4</sub> – 1 mM KCl solution shown in Figure 3. With a constant 0.1 mM K<sub>2</sub>SO<sub>4</sub> content, the molarity of potassium chloride was varied -- 0.0001



M, 0.001 M, 0.01 M, 0.1 M KCl content – resulting in a similar slope which is related to the polarization resistance (Eq. 1), as shown in Figure 3. The steeper the slope, the greater the polarization resistance, and inversely related to the corrosion rate. The effect of a stagnant, stirred and N<sub>2</sub> injected solution on the LPR measurement for a 0.1 mM KCl solution is shown in Figure 4. For the unstirred solution, stirred solution and N<sub>2</sub> injection into solution, the effect of the KCl content on the LPR data are shown in Figures 5-7. The nitrogen injection increased the slope and narrowed the range of current density (Figure 7).

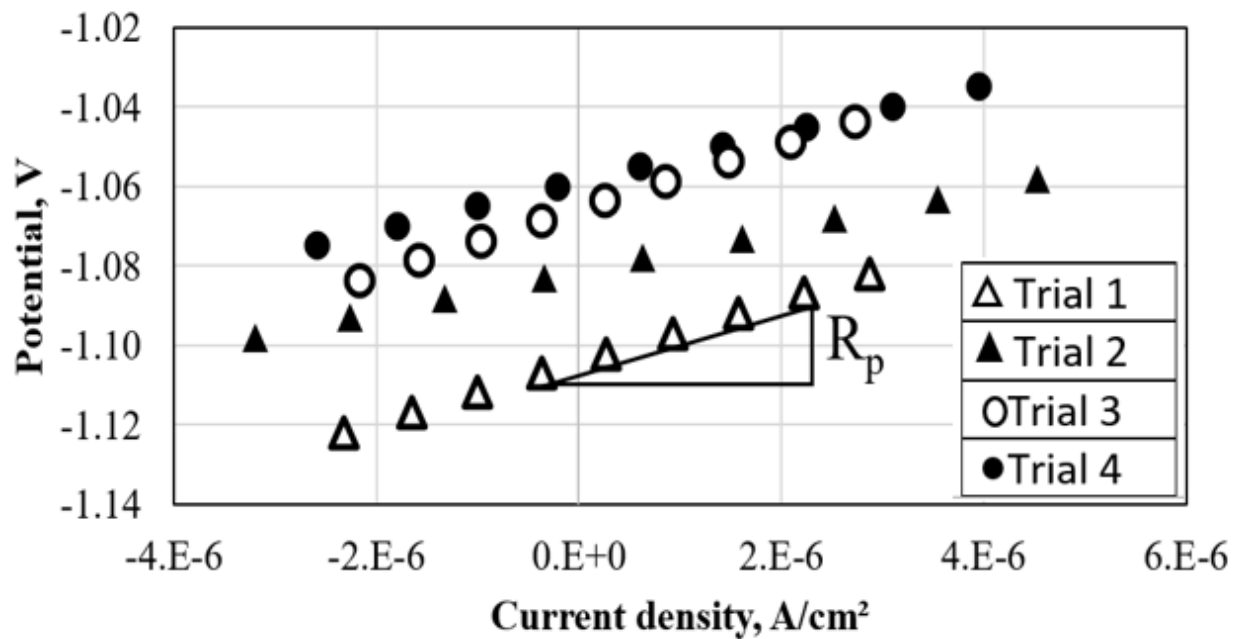


Figure 3 - Four trials of LPR measurements for a 0.1 mM K<sub>2</sub>SO<sub>4</sub> - 1 mM KCl Solution

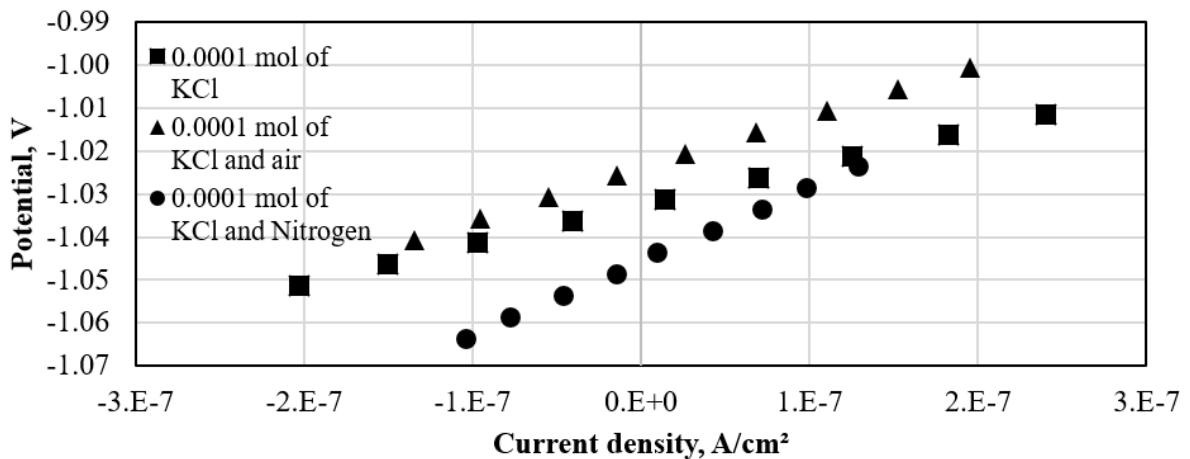


Figure 4 - LPR Plots for 0.1 mM  $K_2SO_4$  - 0.1 mM KCl for a stagnant, stirred and  $N_2$  injected

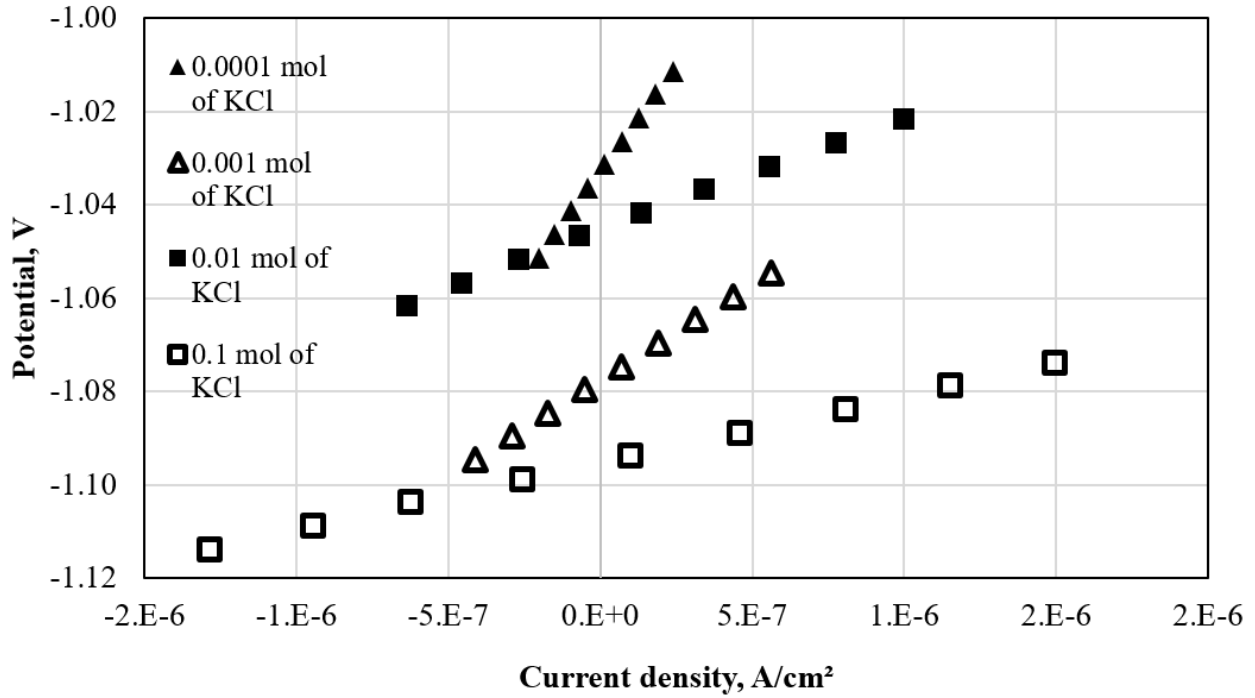


Figure 5. - The effect of KCl content additions on the LPR measurement in a stagnant 0.1 mM  $K_2SO_4$  stagnant solution

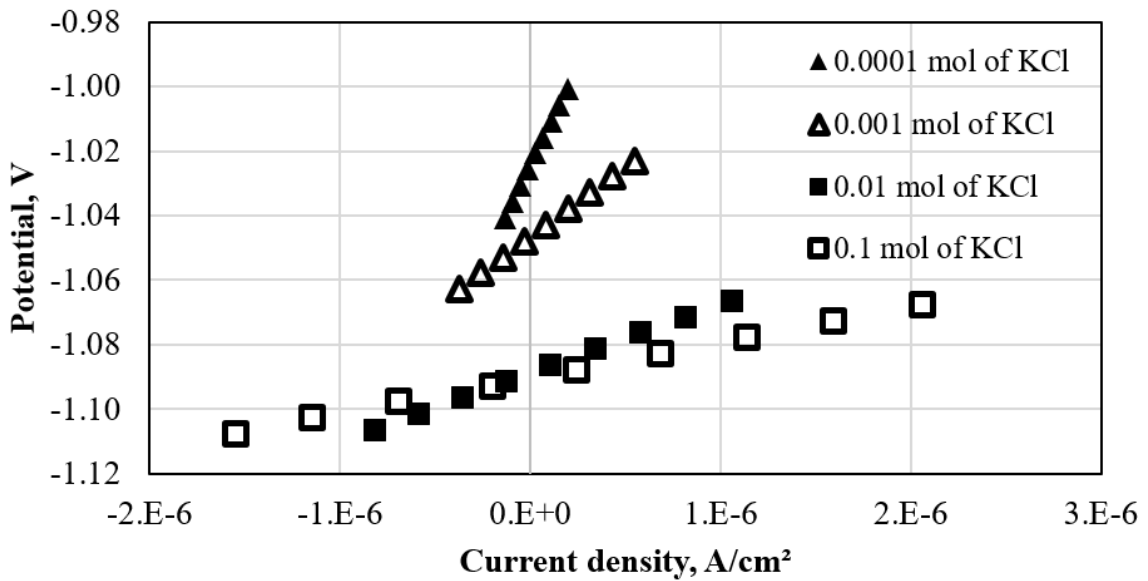


Figure 6. - The effect of KCl content on the LPR measurement in a stirred 0.1 mM  $K_2SO_4$  solution

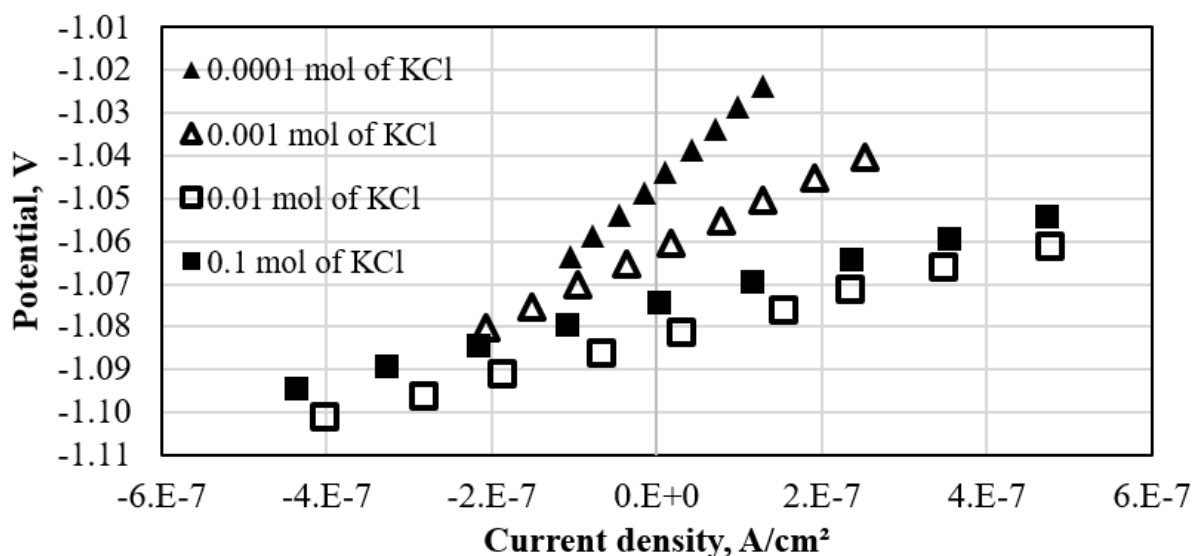


Figure 7 - The effect of KCl solution on the LPR measurement in a 0.1 mM  $K_2SO_4$  solution injected with  $N_2$

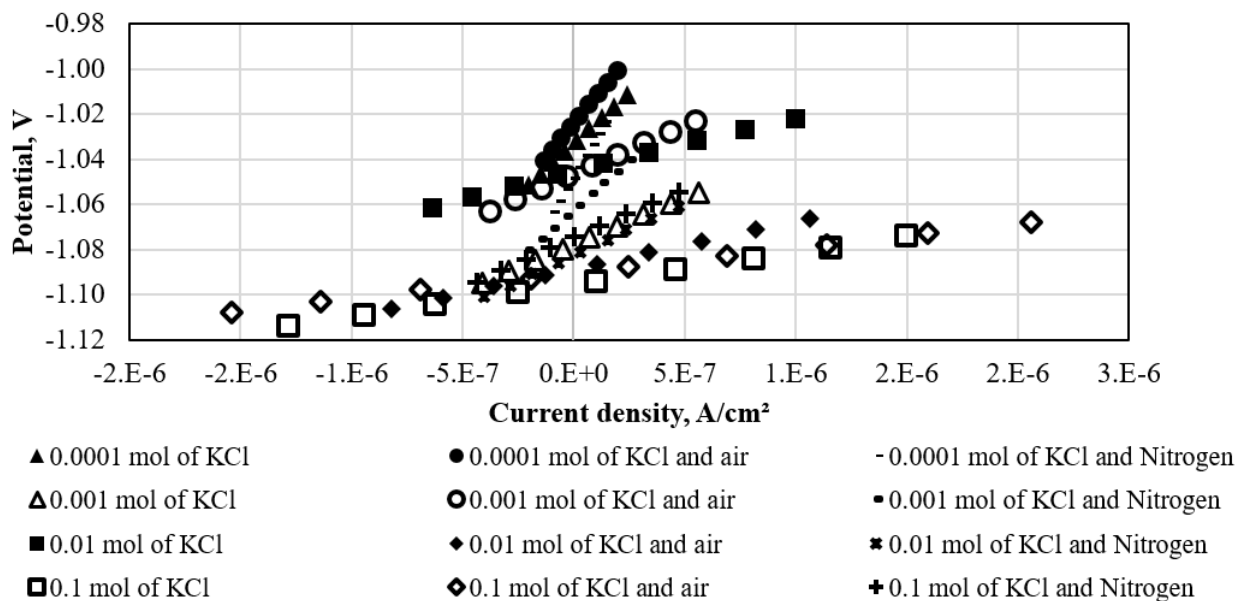


Figure 8 - Comparison of stagnant, stirred and  $N_2$  injected solutions for KCl- 0.1 mM  $K_2SO_4$  solutions

For comparison purposes, every molarity and atmosphere tested are shown in Figure 8. The flattest slope of the LPR plot is 0.1 M KCl solution mixed with air, which was drawn into the solution by simply stirring it. This is easy to spot by how the points are spread away from one another.

### Acquisition of Tafel Data

Four trials of Tafel plots for a mixture of 1 mM KCl and 1 mM K<sub>2</sub>SO<sub>4</sub> were acquired as shown in Figure 9. The same procedure was done for each molarity under stagnant, stirred and N<sub>2</sub> injected 0.1 M KCl solutions. Also, Tafel slopes were acquired within a 130 mV range from the corrosion potential ( $E_{\text{corr}}$ ) represented by the cusp of the curves rendered by the anodic and cathodic sides of the potential-current scan (or polarization scan), as shown in Figure 9.

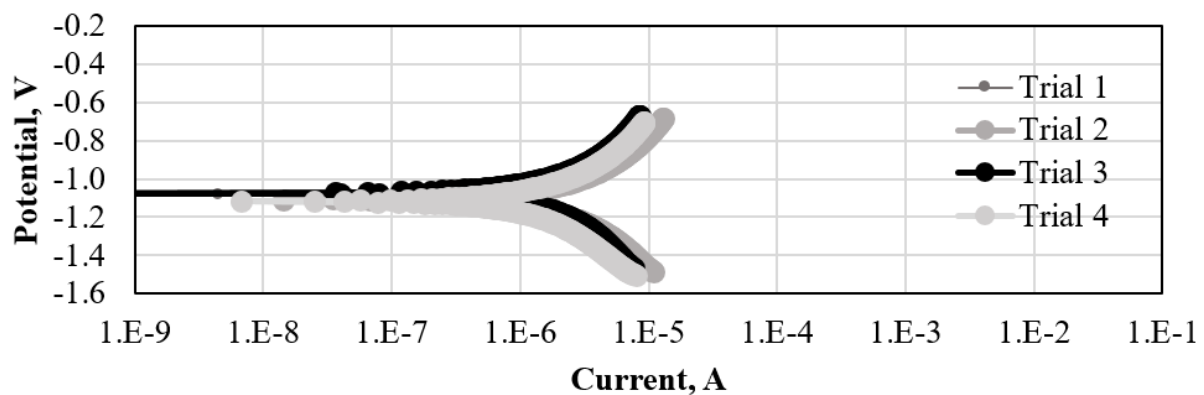


Figure 9. - Four trials of a Tafel plot 0.1 mM K<sub>2</sub>SO<sub>4</sub> - 0.1 mM KCl for a stirred condition

The anodic and cathodic slopes intersect at the corrosion current which is directly related to the corrosion rate. Hence, the movement or shifting of the polarization scan to change the current or current density sufficiently affects the corrosion rate, as evident in Figure 10. The mixing of air and N<sub>2</sub> by having solutions under stagnant, stirred and N<sub>2</sub> injection suggests a decreasing corrosion rate. The nitrogen injection to the solution irrespective of the KCl content shifts the polarizing scans to the left or to decreasing current. If one considers the stagnant solution as a baseline, the drawing of air into the solution will have more dissolved oxygen affecting Zn oxidation, or the anodic reaction,

and decreases the mass transfer of oxygen enabling the dissolved oxygen in the solution to increase slightly for the cathodic reaction.

The polarization scans shift to the right, or the corrosion current increases, with increasing KCl molarity, as shown in Figures 11-13. In addition, the scans decrease slightly as exemplified by the corrosion potential decreasing with increasing chloride content. The same trend of the polarizing scans for 0.1 mM  $K_2SO_4$  shifting with the atmosphere for KCl contents ranging from 0.1 mM to 0.1 M KCl is shown in Figure 14.

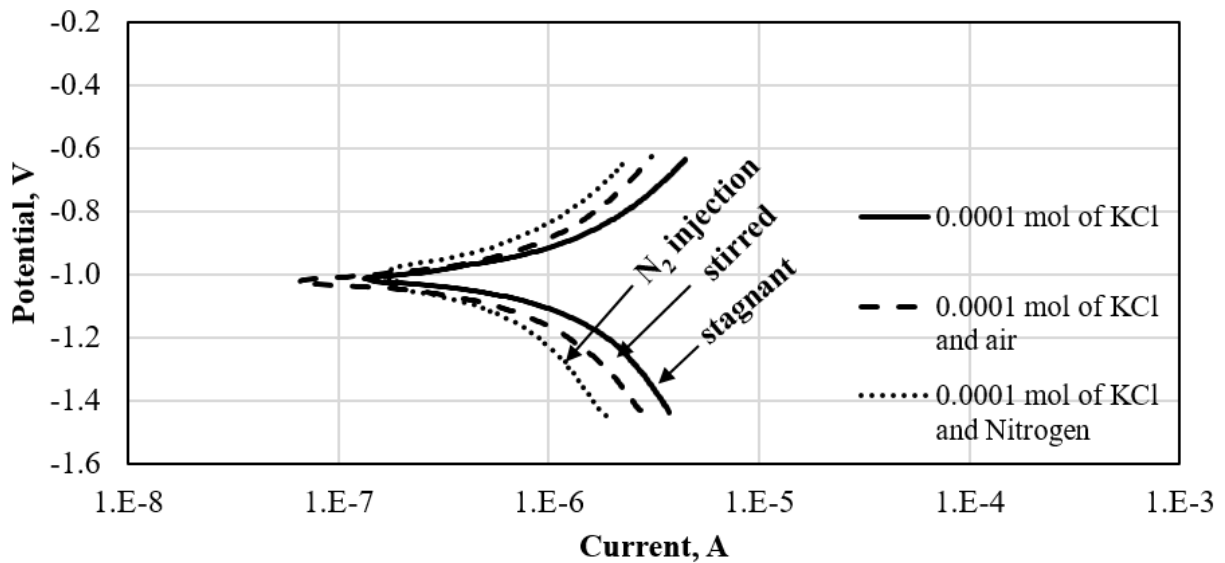


Figure 10 - Four trials of a Tafel plot 0.1 mM  $K_2SO_4$  - 0.1 mM KCl for a stirred condition

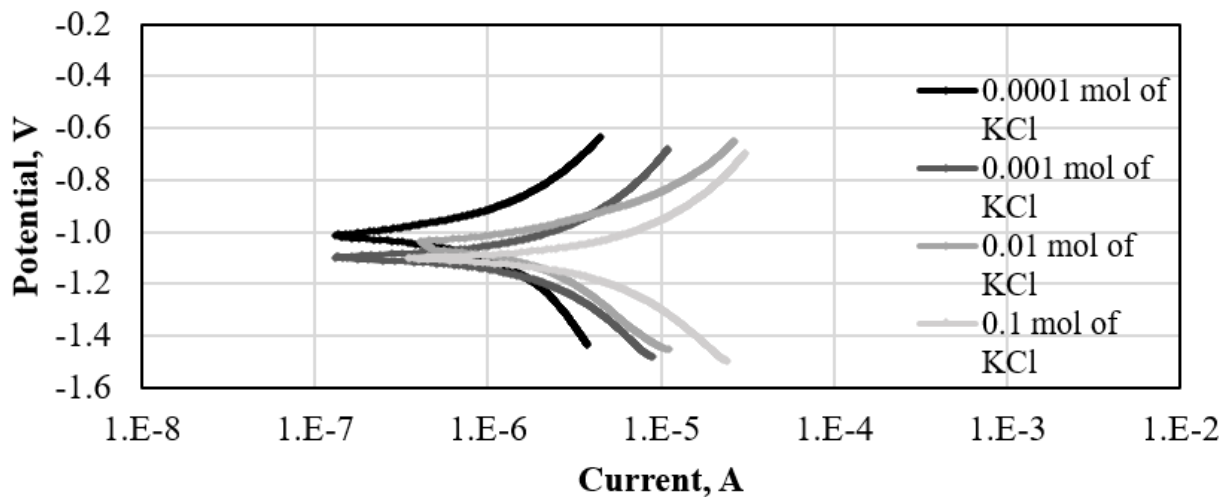


Figure 11 - Tafel plots comparison of changing atmosphere by having a stagnant, stirred and  $N_2$  injected 0.1 mM  $K_2SO_4$  - 0.1 mM KCl solution

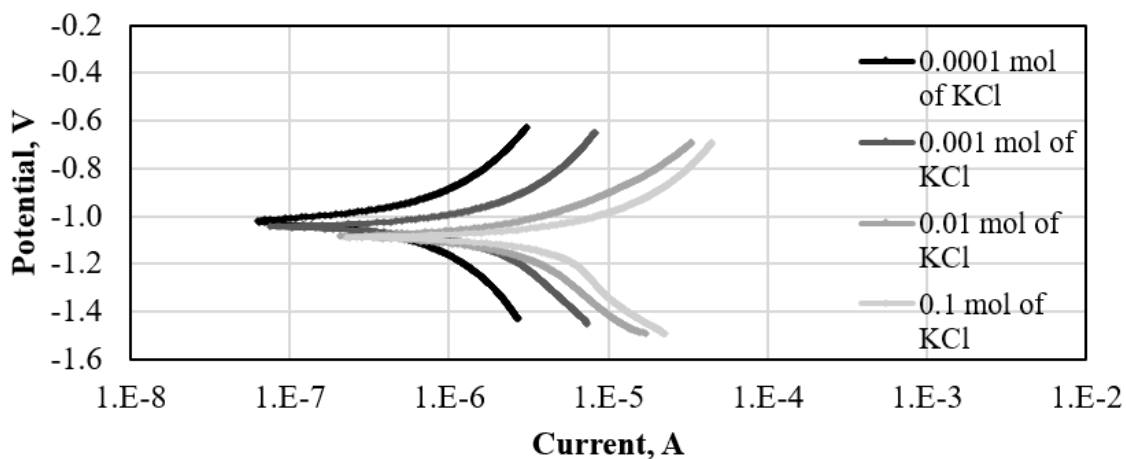


Figure 12. - The effect of KCl solution on the Tafel plot in a stagnant 0.1 mM  $K_2SO_4$  solution

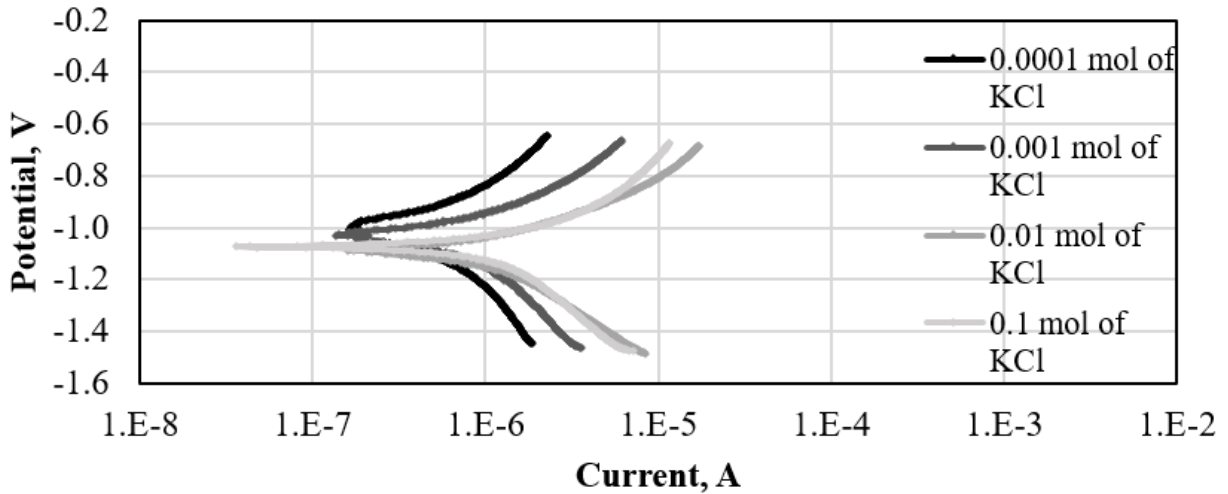


Figure 13 - The effect of KCl solution on the Tafel plot in a 0.1 mM  $K_2SO_4$  solution injected with  $N_2$

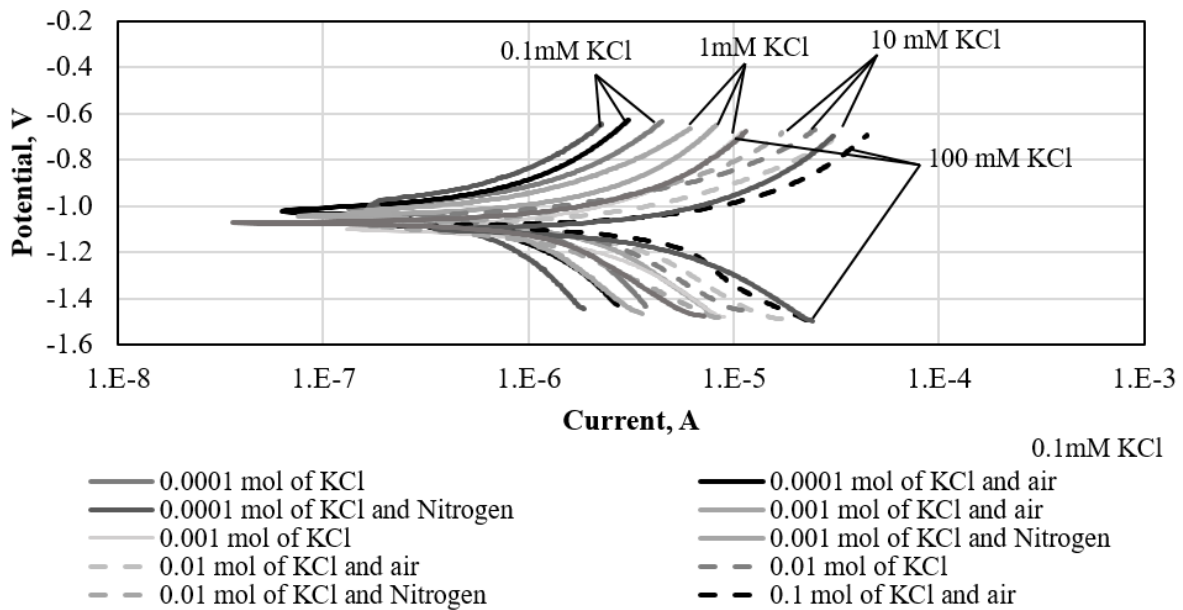


Figure 14 - Comparison of stagnant, stirred and  $N_2$  injected solutions for KCl- 0.1 mM  $K_2SO_4$  solutions

### Analysis Relating Resistivity to Corrosion Rate

An analysis was developed to correlate the resistivity of KCl or KCl- $K_2SO_4$  solutions to the corrosion rate of galvanized steel. The resistivity's were obtained after performing electrochemical measurements for each solution. Since the chloride content

is related to the resistivity and the chloride content directly affects the corrosion rate of galvanized steel, then the resistivity should infer a direct relationship with the corrosion rate. Three techniques were used to calculate the corrosion rate – one with the Tafel slopes within 130 mV range of the  $E_{\text{corr}}$  (denoted as Tafel), the second method combined Tafel slopes determined within 130 mV of  $E_{\text{corr}}$  and LPR (labeled as LPR CR) and the third method used the Tafel slopes within 110 mV range from  $E_{\text{corr}}$  combined with LPR (labeled as LPR CR selected). The corrosion rates are depicted in Figures 15-121 and the data are also appended.

The resistivity of stagnant KCl solutions decreased with increasing KCl content though the 0.01 and 0.1 M KCl appears to reach a plateau, as shown in Figure 15. Similarly, the corrosion rates of the galvanized steel immersed in KCl solutions as a function of molarity are summarized according to Tafel CR, LPR CR and LPR CR selected, as shown in Figure 16. By relating the molarity with resistivity and corrosion rate, a function was acquired to correlate the resistivity to the corrosion rate, as shown in Figure 17.

The effect of the KCl content on the resistivity of stirred KCl solutions is shown in Figure 18. The follow-up of the correlation of the resistivity to the corrosion rate of the stirred KCl-0.1 mM  $\text{K}_2\text{SO}_4$  solutions is shown in Figure 19. Similarly, the effect of KCl content on the resistivity of KCl-0.1 mM  $\text{K}_2\text{SO}_4$  solutions injected with  $\text{N}_2$  is shown in Figure 20. The corresponding correlation of the resistivity with the corrosion rate KCl-0.1 mM  $\text{K}_2\text{SO}_4$  solutions injected with  $\text{N}_2$  is shown in Figure 21.

For the three atmospheric conditions of stagnant, stirred and injected nitrogen, the resistivity vary slightly though the corrosion rate is visibly distinguished. The effect of the atmospheric condition suggests that macrocells may develop along the length of the galvanized strip, especially when corroding at differing rates. The varying oxygen content on the Zn coating of the galvanized steel may change the characteristics of the corrosion products affecting further the corrosion rate.



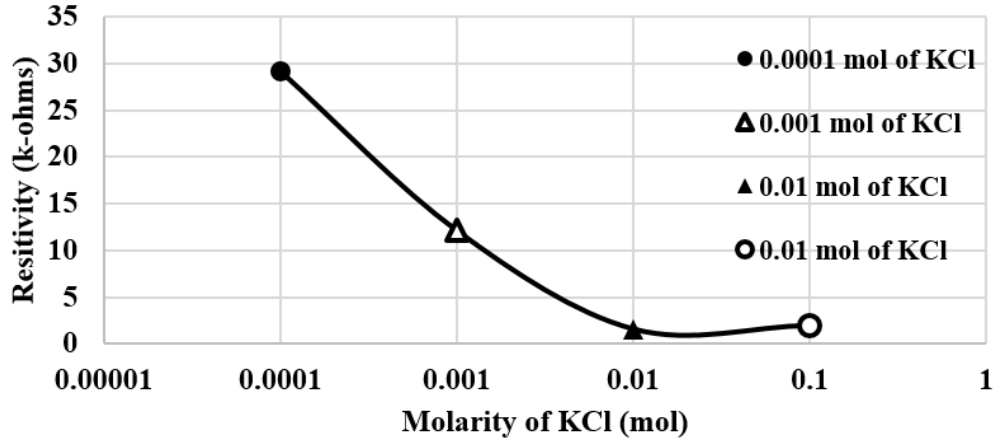


Figure 15 - The effect of KCl content on the resistivity of a stagnant solution KCl- 0.1Mm  $K_2SO_4$  solutions

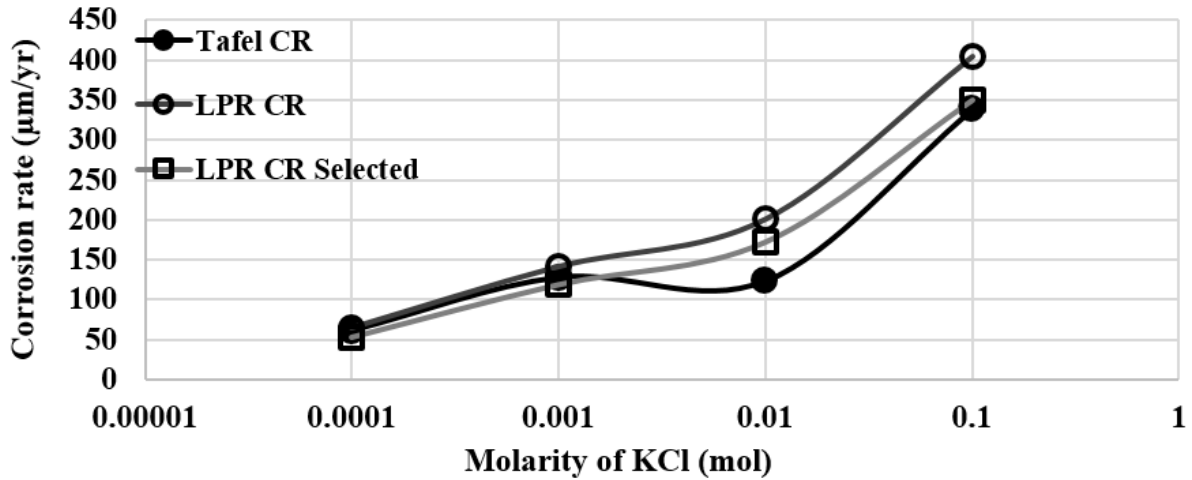


Figure 16 - The effect of KCl content on the corrosion rate determined with Tafel, and LPR techniques for stagnant KCl- 0.1 Mm  $K_2SO_4$  solutions

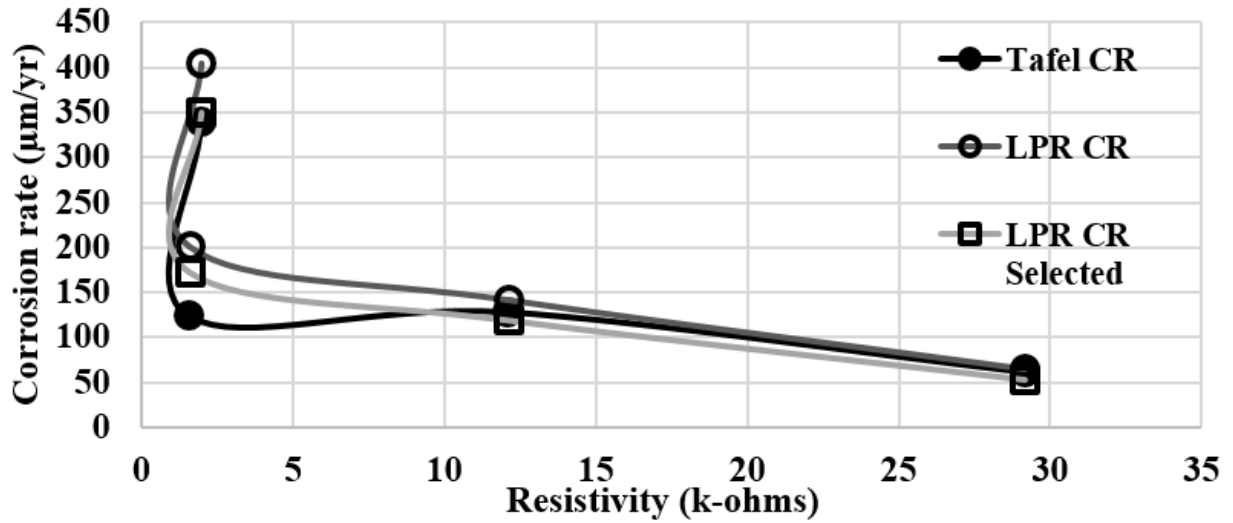


Figure 17 - The correlation of the resistivity with the corrosion rate of stagnant KCl-0.1mM K<sub>2</sub>SO<sub>4</sub> solutions

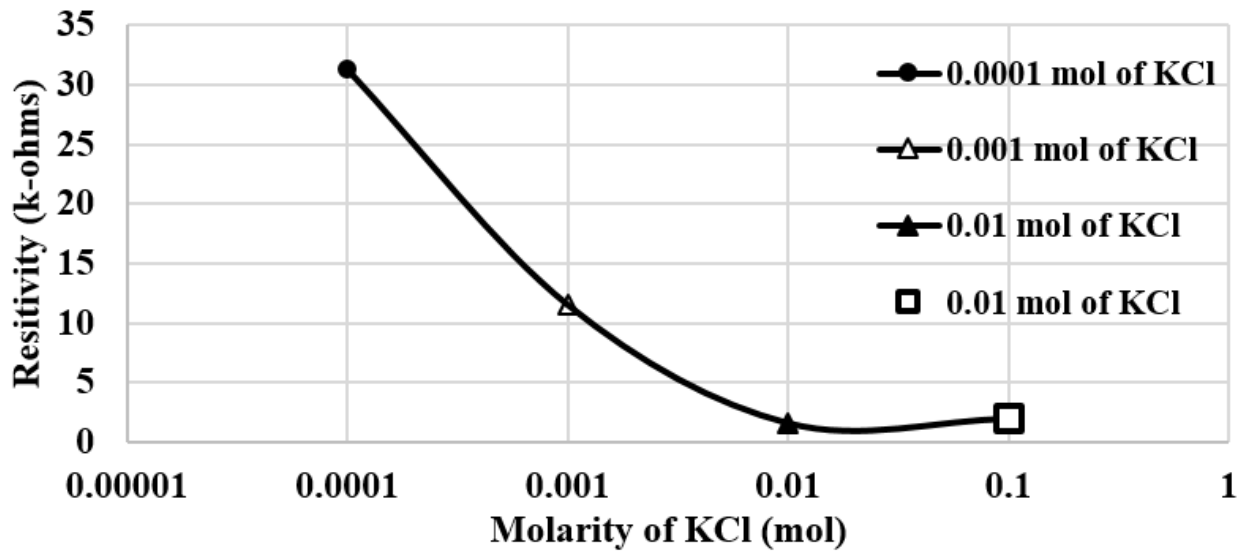


Figure 18 - The effect of KCl content on the resistivity of a KCl - 0.1 mM K<sub>2</sub>SO<sub>4</sub> stirred solutions

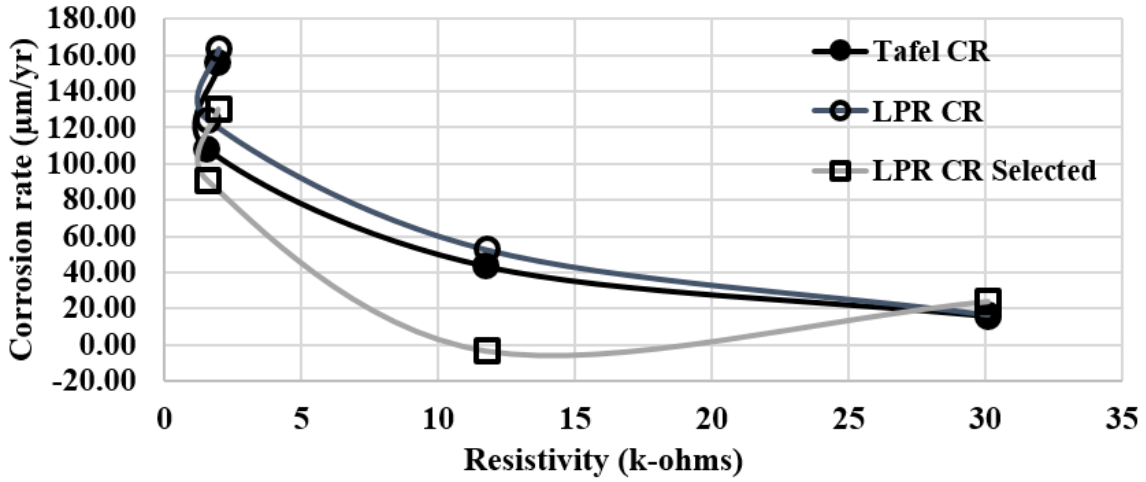


Figure 19. - The correlation of the resistivity with the corrosion rate determined with Tafel and LPR techniques for stirred KCl- 0.1mM K<sub>2</sub>SO<sub>4</sub> solutions injected with N<sub>2</sub>

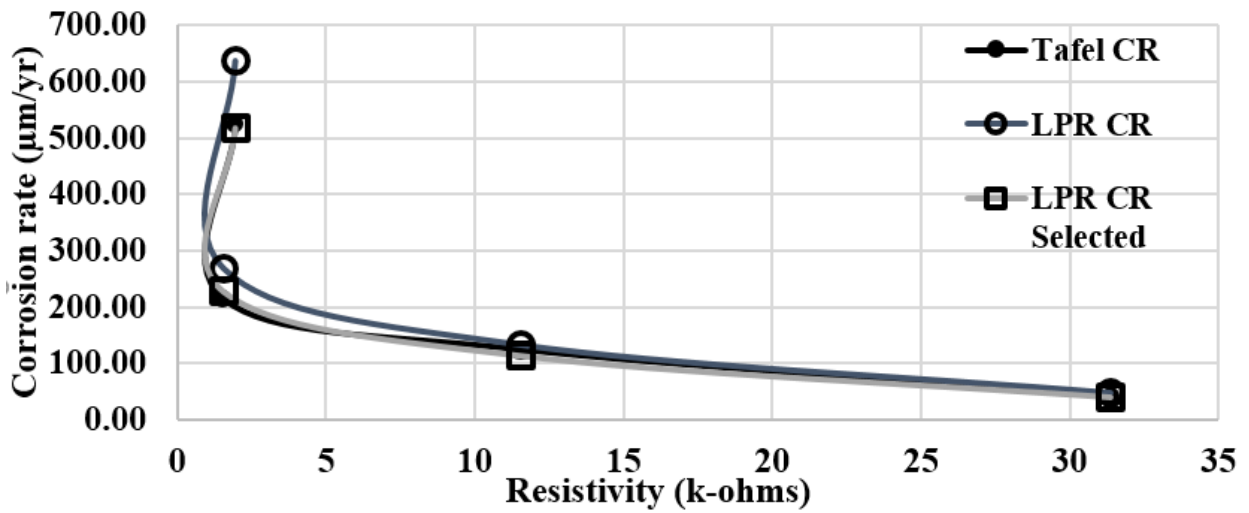


Figure 20 - The effect of KCl content on the resistivity of a KCl molarity- 0.1 mM K<sub>2</sub>SO<sub>4</sub> injected N<sub>2</sub> solutions

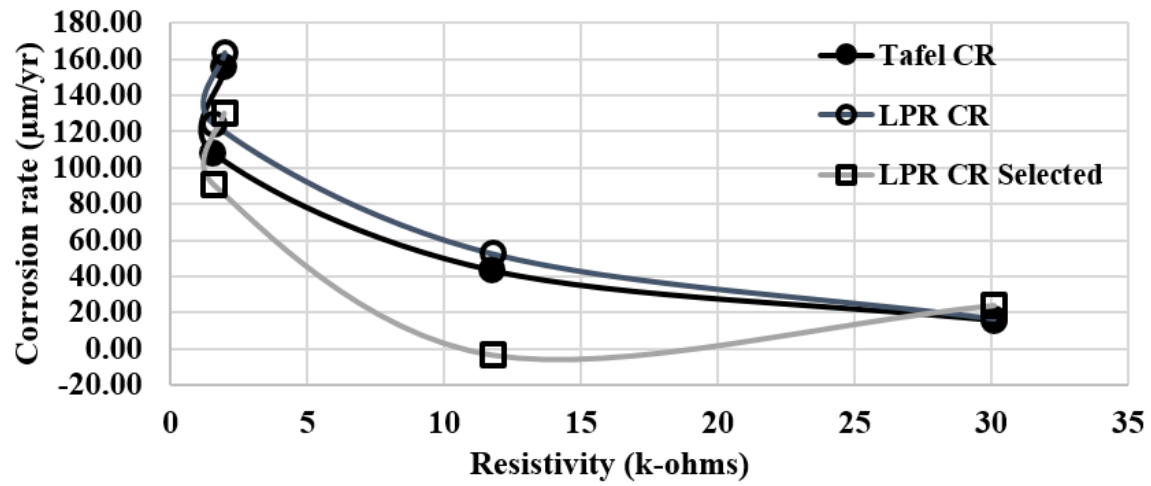


Figure 21 - The correlation of the resistivity with the corrosion rate determined with Tafel and LPR techniques for stirred KCl- 0.1mM K<sub>2</sub>SO<sub>4</sub> solutions injected with N<sub>2</sub>

## Summary

Mechanically stabilized earth (MSE) reinforcements composed primarily of galvanized steel are embedded in soils varying in corrosion susceptibility depending primarily on the concentration of chloride and sulfate ions within the pores of the soil or even the water collected in the backfill. The objective of this study was to link the resistivity to of the KCl-K<sub>2</sub>SO<sub>4</sub> solutions with the corrosion rate of the galvanized steel exposed to these solutions. The corrosion rates were determined with electrochemical measurements consisting of linear polarization resistance (LPR) and Tafel slopes acquired from polarization scans. Three techniques were used to calculate the corrosion rate – one with the Tafel slopes within 130 mV range of the E<sub>corr</sub> (denoted as Tafel), the second method combined Tafel slopes determined within 130 mV of E<sub>corr</sub> and LPR (labeled as LPR CR) and the third method used the Tafel slopes within 110 mV range from E<sub>corr</sub> combined with LPR (labeled as LPR CR selected). The three techniques determined consistent corrosion rates of galvanized steel with resistivity though the potential range selected of the Tafel slope seems to affect the corrosion rate calculated.

In addition, the atmospheric condition of the solution does affect slightly the corrosion rate of the galvanized steel for stagnant, stirred and N<sub>2</sub> injected solutions. If one considers the stagnant solution as a baseline, the drawing of air into the solution will have more dissolved oxygen affecting Zn oxidation, or the anodic reaction, and decreases the mass transfer of oxygen enabling the dissolved oxygen in the solution to increase slightly for the cathodic reaction. Although the differential among the corrosion rates caused by the dissolved oxygen may establish macrocells along the length of the galvanized steel, their effect on the overall metal corrosion needs further study.

## **Implementation/Technology Transfer (if applicable)**

## References

1. Borrok D., A. Bronson and S. Nazarian, "Characterization of Coarse Backfill Materials for Prevention of Corrosion MSE Metallic Wall Reinforcement," Research Report FHWA/TX 11/0-6359-1, Texas Department of Transportation, Austin, TX, 2013.
2. Elias V., K.L. Fishman, B.R. Christopher, and R. R. Berg. Corrosion/Degradation of Soil Reinforcements for Mechanically Stabilized Earth Walls and Reinforced Soil Slopes. Report FHWA-NHI-09-087, National Highway Institute, Federal Highway Administration, Washington, D.C, 2009.
3. El-Mahdy, G.A., A. Nishikata, T. Tsuru. (2000) *Electrochemical Corrosion Monitoring of Galvanized Steel under Cyclic Wet-Dry Conditions*. *Corrosion Science*, Vol. 42, pp. 183-194.
4. Fishman, K. L., and Withiam, J. L. (2011). LRFD Metal Loss and Service-Life Strength Reduction Factors for Metal-Reinforced Systems (p. 71, Rep. No. 675). Washington, D.C.: Transportation Research Board.
5. Gladstone, R.A., Anderson P.L., K.L. Fishman, and Withiam J.L. (2006). *Durability of Galvanized Soil Reinforcement: More than 30 Years of Experience with Mechanically Stabilized Earth*. Transportation Research Record: Journal of the Transportation Research Board No. 1975, Transportation Research Board of the National Academies, Washington, D. C., pp. 49-59.
6. Jones, D. A. (1992) *Principles and Prevention of Corrosion*, pg. 155-158, Macmillan Publishing Company, New York.
7. Oldham, K and F. Mansfeld. (1973) *Corrosion Rates from Polarization Curves: A New Method*. *Corrosion Science*, Vol. 13, pp. 813-819
8. Sagues, A., R. Scott, J. Rossi, J. A. Peña and R. Powers. (2000) *Corrosion of Galvanized Strips in Florida Reinforced Earth Walls*. *Journal of Materials in Civil Engineering*, Vol. (8), pp. 220-227.

9. Yadav, A.P., A. Nishikata, T. Tsuru. (2004) *Degradation Mechanism of Galvanized Steel in Wet-Dry Cyclic Environments Containing Chlorides*, *Corrosion Science*, Vol. 46, pg. 361-376,



## Appendix

**Table 1. Tafel corrosion rates dependent on gas flushing conditions**

Gas Flushing	icorr Average (A/cm <sup>2</sup> )	icorr SD (A/cm <sup>2</sup> )	Coefficient of Variance	Tafel CR (μm/yr)
Nitrogen	1.02E-06	1.93E-06	188%	15.34
air	2.82E-06	5.23E-07	19%	42.16
none	4.10E-06	1.60E-06	39%	61.35

**Table 2. Average Tafel corrosion rates for every condition and molarity**

Gas Flushing	KCl molarity (mol)	icorr Average (A/cm <sup>2</sup> )	icorr SD (A/cm <sup>2</sup> )	Coefficient of Variance	Tafel CR (μm/yr)
Nitrogen	0.0001	1.02E-06	1.93E-06	1.88	15.34
air	0.0001	2.82E-06	5.23E-07	0.19	42.16
none	0.0001	4.10E-06	1.60E-06	0.39	61.35
Nitrogen	0.001	2.87E-06	4.99E-07	0.17	42.99
Air	0.001	8.32E-06	2.27E-06	0.27	124.52
None	0.001	8.54E-06	1.36E-06	0.16	127.80
Nitrogen	0.01	7.19E-06	5.04E-06	0.70	107.69
Air	0.01	1.43E-05	9.36E-06	0.66	213.80
None	0.01	8.25E-06	7.24E-07	0.09	123.55
Nitrogen	0.1	1.04E-05	6.70E-06	0.65	155.28
Air	0.1	3.51E-05	4.65E-06	0.13	525.37
None	0.1	2.26E-05	8.14E-06	0.36	338.24

**Table 3. LPR Data: maximum range of 110 millivolts**

Gas Flushing	KCl molarity (mol)	$i_{corr}$ Average (A/cm <sup>2</sup> )	$i_{corr}$ SD (A/cm <sup>2</sup> )	Coefficient of Variance	LPR CR (μm/yr)
Nitrogen	0.0001	1.59E-06	4.27E-07	0.27	23.86
air	0.0001	2.70E-06	4.99E-07	0.18	40.41
none	0.0001	3.55E-06	1.74E-06	0.49	53.17
Nitrogen	0.001	-2.35E-07	4.59E-06	-19.55	-3.52
Air	0.001	7.60E-06	7.57E-06	1.00	113.82
None	0.001	7.94E-06	1.44E-06	0.18	118.92
Nitrogen	0.01	6.06E-06	2.75E-06	0.45	90.71
Air	0.01	1.52E-05	7.21E-06	0.48	227.02
None	0.01	1.15E-05	3.69E-07	0.03	172.15
Nitrogen	0.1	8.69E-06	5.75E-06	0.66	130.04
Air	0.1	3.45E-05	1.01E-05	0.29	516.90
None	0.1	2.33E-05	4.91E-06	0.21	349.40

**Table 4. LPR Data: maximum range of 130 millivolts**

Gas Flushing	KCl molarity (mol)	$i_{corr}$ Average (A/cm <sup>2</sup> )	$i_{corr}$ SD (A/cm <sup>2</sup> )	Coefficient of Variance	LPR CR (μm/yr)
Nitrogen	0.0001	1.11E-06	2.03E-06	1.83	16.64
air	0.0001	3.23E-06	6.08E-07	0.19	48.34
none	0.0001	4.32E-06	2.17E-06	0.50	64.70
Nitrogen	0.001	3.50E-06	9.73E-07	0.28	52.45
Air	0.001	3.23E-06	6.08E-07	0.19	48.34
None	0.001	9.44E-06	1.70E-06	0.18	141.27
Nitrogen	0.01	8.28E-06	4.74E-06	0.57	123.91
Air	0.01	1.80E-05	9.28E-06	0.52	269.11
None	0.01	1.34E-05	2.04E-07	0.02	200.58
Nitrogen	0.1	1.09E-05	7.74E-06	0.71	163.31
Air	0.1	4.26E-05	1.12E-05	0.26	637.91
None	0.1	2.70E-05	6.19E-06	0.23	404.04